Eyelid Gesture Control using Wearable Tunnelling Magnetoresistance Sensors

Asfand Tanwear, Elvira Paz, Tim Böhnert, Ricardo Ferreira, Hadi Heidari
Microelectronics Lab (meLAB), James Watt School of Engineering, University of Glasgow, G12 8QQ, UK
International Iberian Nanotechnology Laboratory (INL), 4715-330 Braga, Portugal

***Abstract*—Everyday technologies are more than ever digitized with internet of thing's systems and disabled individuals may feel excluded. Handsfree gesture approaches such as eye movements/blinking can enhance the interacting with modern technology. This work presents eye blinking for eyelid gesture control using a wearable magnetic system consisting of a flexible magnetic strip on the eyelid and spintronic magnetic sensors with its analogue front-end circuit. To detect eye blinking, tunnelling magnetoresistance (TMR) sensors with sensitivity of 11mV/V/Oe are embedded into an eyeglass frame. For successful detection of the small magnetic field generated by 6 mm diameter with 1 mm thickness magnetic strip on the eyelid, a sensor readout circuit is designed to amplify the collected signal and cancel the external noise and offset. The circuit is capable of filtering low frequencies <0.5 Hz and DC offsets. High frequencies above >28 Hz is filtered for both magnetic field and eyelid movement noise. Each TMR sensor circuit is equipped with a fixed-gain amplifier for detecting low-magnetic field from the mm-sized magnetic strips. The blinks can be repeated within a set time frame and since both eyelids will be detected, multiple command combinations are possible for classification. Based on magnetic field simulation results, the circuit was simulated and has shown high repeatability and stability that can classify eyeblinks based on amplitude threshold. As a result, the signal can be scaled and classified on a Bluetooth microcontroller capable of connecting to various Bluetooth enabled devices for the disabled individuals to communicate external technology with.**

Keywords—Spintronics; Tunnelling Magnetoresistance Sensor; Eyelid Control; Human-Machine Interface

I. INTRODUCTION

There are multiple forms of patient rehabilitation methods that allows a patient to interface with the real-world and improve quality of life. A method of interaction can be made from eyeblinks for human-computer interactions and tools such as electrooculogram (EOG) have been used for registering eyeblinks [1]. Where eye-related disorder can be studied for their relationship between eye blinking and eye movement when performing everyday activities, such as sleep quality and sports performance [2]. Alternatively, and increasingly more popular, are the visual-based eye trackers that are able to record eyeblinks and eye movements from a camera for clinical studies instead of EOG [3]. Typically, near infrared (NIR) light transmitters and cameras are used, where Infrared light from the transmitter is reflected from the cornea to the camera and measures pupil to reflection difference[4]. For the advantage of mobility, the mobile eye-trackers using NIR are generally twice as expensive as desktop based NIR ($5000) with the sampling rate and accuracy also reduced [5]. State-of-the-art mobile eye-trackers such as the, 'Tobii Glasses 2', can send data wirelessly for human-computer interface. The glasses are powered via cables, as camera-technology require a constant connection to a large battery from the body mount unit [6].

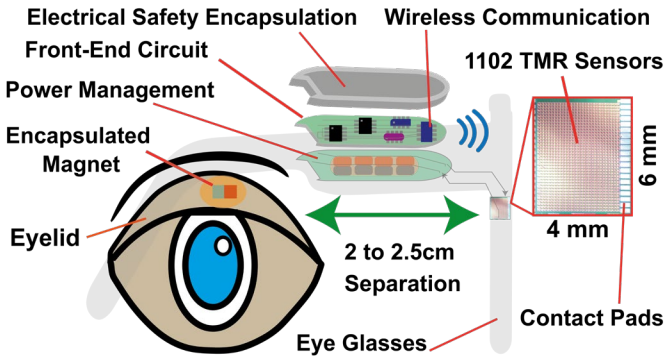

Fig. 1. Magnetic strips are attached to the eyelid and are detected by magnetic sensors 2.5 cm away.

In this paper, an alternative non-visual eyeblink detection method is proposed for wearable applications that will control external electronic devices, as shown in Fig. 1. Whereby, consecutive voluntary eyeblinks can be differentiated from involuntary ones for hands-free commands. The magnetic sensing device is a thin-film solid-state spintronic sensor with the ability to differentiate in-plane field of the single-axis sensor [7]. The tunnelling magneto-resistance (TMR) sensor is generally more sensitive than Anisotropic-Magnetoresistance (AMR) , Giant-Magnetoresistance (GMR) or Hall-effect sensors [8]. The TMR sensors also have comparably lower sensor size and bias current that makes it more compatible for wearable applications [9], [10]. The spintronic TMR sensors operate by altering its device resistance depending on the direction and field strength of the in-plane magnetic field. Where parallel fields have low resistance and high resistance when the in-plane field is anti-parallel to the pinned layer[11].

The proposed system requires a simulation model to test the analogue front-end (AFE) circuit of the TMR sensors. In addition, the magnetic field from the magnetic strip on the eyelid is simulated with respect to the distance to the sensor. With the known sensor's performance and simulated magnetic field, the circuit performance can be approximated. The aim of the circuit simulation is to analyse signal stability and signal loss for eyelid detection. In this paper, the simulation's methodology is

followed by results and discussion, with summation of the paper in the conclusion.

II. Methodology

A. Tunneling Magnetoresistance Chip on Eyeglasses

The 6 x 5 x 1 mm^3 spintronic magnetic sensor chip consists of 1102 series double-pinned TMR stack with aluminium contact pads connecting to the front-end circuit [12]. The sensor offers magnetoresistance ratio performance of 112% with sensitivity at 11 mV/V/Oe, this is based on chip characterization tests and will serve as a reference device for the simulation [13]. The magnet within the eyelid is approximately 2.5 cm away from the sensor and is centred on the wearable eyeglasses. This is based on preliminary testing from eyeglass users with different eyewear designs and was found that 2.5 cm was the maximum measured separation between the eye lid and the eyeglass frame, with 2 cm average.

B. Eyeblink: Operation and Frequency Bandwidth

The aim of the system is to detect and differentiate involuntary and voluntary blinking from both eyelids to obtain as many combinations as possible. In other words, combination of right and left blinks at alternating sequences, mixed with both eyelids as a third-input option. A trigger-eyelid command will initialize the system, this will be the user's choice between either the left or right eyelid, as involuntary blinking have been observed in this study to occur at both eyelids together, also using a trigger command has shown to improve accuracy [14]. Another option to differentiate any involuntary eyeblinks is by increased blinking speeds than involuntary speeds. From literature, the frequency of involuntary blinking is approximated to be below 0.3 Hz [15]. This implies that involuntary blinking is found in low frequencies. Since voluntary blinks speeds are user determined, and based on preliminary tests, >1 Hz was often achievable as it relates to 1 blink per second and beyond.

C. Magnetic Source Simulation

ANSYS Discovery AIM 2020 V. R1 software is used to determine the in-plane magnetic field of the TMR sensor. This is dependent on the strength of the source magnet and separation between source and sensor. The sensors will detect millimetre(mm) sized magnetic strips attached onto upper eye lid crease, sized around <6.5 mm [16]. Where a N35-Neodymium-Iron (NdFe) magnet with 6 mm diameter and 1 mm thickness are encapsulated in a biocompatible, soft and flexible polydimethylsiloxane (PDMS) strip [17], with self-adhesion it will be placed on both eyelids for wearable applications, as shown in Fig. 2(a). Within the simulation, the permanent magnet is encapsulated by air as the PDMS is assumed to have the same magnetic permeability [18]. Furthermore, with sensitivity of 11 mV/V/Oe (1 Tesla= 10,000 Oe) means the output voltage can be approximated based on the magnetic field at the sensor's position and can provide a criterion for the minimum field required at the source. However, the strength of the magnetic element is limited for safety since, the International Commission on Non-Ionizing Radiation Protection (ICNIRP), has outlined a body exposure limit for the public set at 400 milli-Tesla [19].

D. Analog Front-End Circuit Design

Frequency AC sweep and time domain transient analysis was performed using OrCAD Capture V17.4 to simulate the AFE circuit design, as shown in Fig. 2(c).

Input & High Pass Filter: To represent the input within the circuit model, a signal generator at 3 Hz, 50 mV amplitude and 2.5 VDC offset was used. This is to substitute for the tunnelling magnetoresistance sensor in series with a nominal value matched resistor of 1.75 KΩ (Rx). The input is followed by a 1st-order passive high pass filter at cut-off frequency of 0.5 Hz. The RC passive filter removes input DC offset and low frequency noise <0.5 Hz.

Amplifier & Low Pass Filter: For each TMR sensor, the output response is amplified to increase signal amplitude for

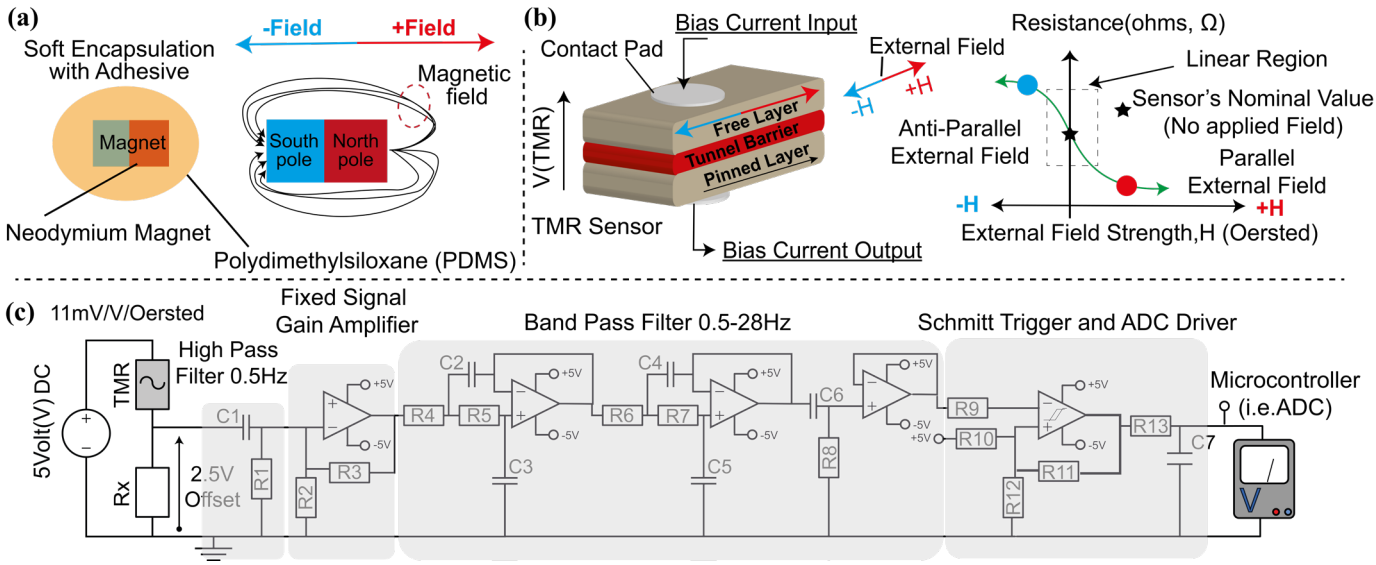

Figure 2. (a) Closeup of dipole magnet encapsulated within soft polydimethylsiloxane (PDMS) material to source magnetic field (b) Current bias flows perpendicular to TMR sensor plane. Sensor resistance varies with external field (c) TMR sensor's analogue front-end circuit for eyelid detection.

signal threshold classification. Using a low input noise operational amplifier (OPA227) ensures noise does not envelope the signal during amplification. This is followed by the low pass 4th-order Butterworth active filter with cut-off frequency of 28 Hz. As at 28 Hz means that sensor would need to detect speeds equivalent to 28 blinks a second, which was found hard to achieve in-lab for an individual. Having a small cut-off frequency ensures the amount of data being analysed is small and 50 Hz power line noise and other high frequency electromagnetic noise from the environment reduced therefore, a 4th-order Butterworth low pass active filter is chosen.

Schmitt Trigger *& Microcontroller*: To process and convert the output signal for classification can be accomplished by a Bluetooth enabled microcontroller. If the controller has a 5 V analogue-to-digital (ADC) input limit, then a positive signal polarity from 0 V to 5 V are accurately processed and outside this range may damage the input pins of the device. A Schmitt trigger is converting the analogue signal amplitude of <0.3 V threshold to 0V and >1.3 V to 5 V. This results in a binary input to the microcontroller and then programmed depending on the pattern being received to control external device via Bluetooth. For protection, a single supply voltage OPAMP (AD8544) for a Schmitt trigger's comparator was used, as it limits the maximum output voltage to the ADC pins. Combined with a low value resistor (100 ohms) and a small capacitor (1nF) can act as an output low pass filter to attenuate very high frequency noise from the OPAMP. As well as, the capacitor acts as reservoir of charge and the resistor to limit peak transient currents [20].

III. Results and Discussion

A. Magnetic Field at Sensor Result

Fig. 3(a). and 3(b). shows the simulation results of the magnetic field from the eyelid to the sensor's position. Where a N35-NdFe permanent magnet with a maximum flux density of 1.089 T (1.08 KOe) at the source and 2.5 cm away is the sensor at minimum field of 0.07 mT (0.7 Oe). And Fig. 3(b). shows a graph results as expected, as field strength is decreased nonlinearly at a one over the cubed rate per unit distance [21]. For the TMR sensor, at 2.5 cm (0.7 Oe) from the source would result in approximately 7.7 mV per voltage bias when sensitivity is at 11 mV/V/Oe. The TMR sensor would require amplification and/or an increase in sensor's voltage bias to output a larger amplitude for classification. Since, the circuit system is already supplied at ± 5 V means the TMR sensor with 5 V bias can increase sensitivity to 38.5 mV/Oe and produce 27 mV amplitude at 0.7 Oe. This is possible as the sensor is shown to increase bias voltage up to 20 V and maintaining sensitivity at the expense of increased sensor noise floor but not enough to drown the relatively high fields from the eyelid. Furthermore, if the amplifier were set to a gain of 40(+32 dB), the output amplitude can reach 1 V, this is would be plenty sufficient amplitude for threshold classification systems. Alternatively, if the design of eyeglasses can be altered to bring separation of eyelid closer down to 2 cm then the output voltage at 5 V bias would result in the front-end at 87 mV from a 1.59 Oe field and

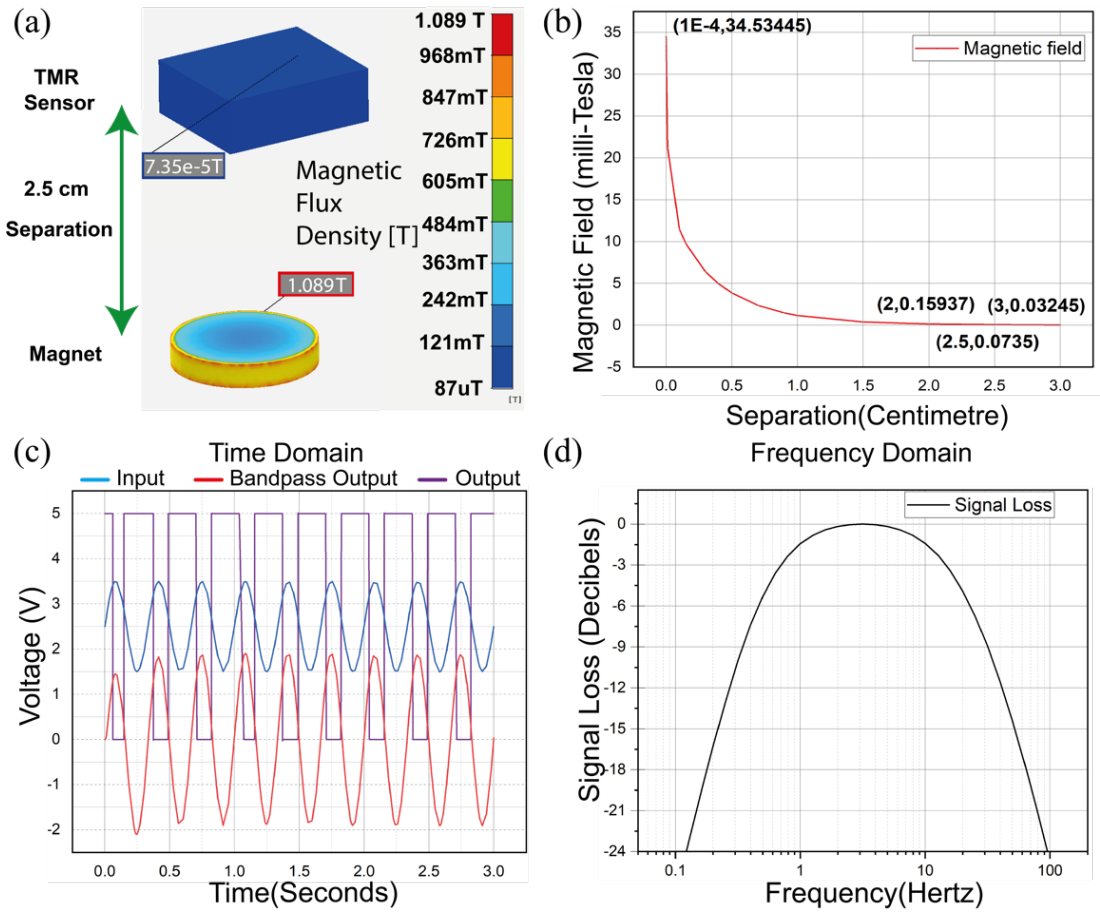

Figure 3. (a) Sensor (blue) with minimum flux density of 73micro-Tesla from magnet with maximum field of 1 T, on surface. (b) Inverse square graph of sensor field against separation of sensor and magnet. (c) Time domain response of output signal (purple), with bandpass filter output (red) and input signal (blue) at 3 Hz. (d) Normalised signal loss response of output signal in frequency domain. Design cut-off frequency at -6 dB points are 0.5 Hz and 28 Hz.

require less need for amplification, as higher gain also inadvertently amplify sensor noise.

B. Front-End Circuit Stability & Signal Loss Results

In Fig. 3(c). shows the time domain response of the signal output binary output between maximum voltage 0 to 5 V. This means, for circuit fabrication, the following design can be used as the filtering, amplification and binary output was produced as expected for threshold-based classification. When inspecting the output signal response of the system prior to Schmitt triggering, the signal at the bandpass output is not as smooth as the input, and for signal classification this may reduce the overall accuracy slightly, as the signal output does not exactly represent the input. Furthermore, due to the presence of capacitors causing minor delay issues within the system a transient response is also witnessed at start-up. This is seen as the maximum peak value of each wave is increasing between 0 to 0.5 seconds but will stabilise after the initial 0.5 seconds at the start-up of the system. In Fig. 3(d). shows the frequency response of the front-end blink detection circuit with a -6 dB point at 0.5 Hz and 28 Hz to represent signal loss. As the graph is normalized to show signal loss, the -3 dB cut-off points correlate to 0.5 Hz and 28 Hz as intended, and at 3 Hz the signal will be at +3 dB corresponding to the amplifiers gain of two, as designed. If the TMR sensor can provide a signal amplitude of >50 mV from each eyeblink, then the circuit simulation results will be the same as when the circuit is fabricated. This is possible with a 5 V sensor bias, amplification, and/or an increased source field strength, for example by decreasing separation down to 2 cm. Additionally, using a stronger magnetic material would allow a decrease in size of magnet. If <1.4 mm diameter magnet is used [16] , i.e. the size of the eyelid when open (pretarsal skin crease) would mean a less obtrusive magnetic strip. In summation, the circuit response both within time and frequency domains are as designed and can operate for blink detection.

IV. CONCLUSION

In this paper, we showcased proof-of-concept of a wearable spintronic system with TMR magnetic sensor to detect eyelid movements. The $6 \times 5 \times 1$ mm^3 TMR sensor with sensitivity of 11 mV/V/Oe make it a suitable choice for wearable field sensing of the encapsulated magnet placed on the eyelid. A front-end circuit with a bandpass filter consisting of a high and low pass filters ensures the signal is isolated from magnetic field noise and a user's involuntary blinking whilst, amplifying the signal for improved signal classification. The circuit simulation of the front-end circuit has shown good signal stability for blinking classification. Supported by magnetic simulation, that provided an insight on the magnetic field detected by the TMR sensor when at separation of 2.5 cm away, show blink detection is possible by magnetic sensors and eyelid magnets.

REFERENCES

[1] S. He and Y. Li, 'A Single-Channel EOG-Based Speller', *IEEE Transactions on Neural Systems and Rehabilitation Engineering*, vol. 25, no. 11, pp. 1978–1987, Nov. 2017, doi: 10.1109/TNSRE.2017.2716109.

[2] Y. Cheung and Q. Peng, 'Eye Gaze Tracking With a Web Camera in a Desktop Environment', *IEEE Trans. Human-Mach. Syst.*, vol. 45, no. 4, pp. 419–430, Aug. 2015, doi: 10.1109/THMS.2015.2400442.

[3] V. K. Jaswal, A. Wayne, and H. Golino, 'Eye-tracking reveals agency in assisted autistic communication', *Scientific Reports*, vol. 10, no. 1, p. 7882, May 2020, doi: 10.1038/s41598-020-64553-9.

[4] A. Duchowski, *Eye Tracking Methodology: Theory and Practice*, 2nd ed. London: Springer-Verlag, 2007.

[5] S. Dowiasch, P. Wolf, and F. Bremmer, 'Quantitative comparison of a mobile and a stationary video-based eye-tracker', *Behav Res*, vol. 52, no. 2, pp. 667–680, Apr. 2020, doi: 10.3758/s13428-019-01267-5.

[6] H. Yamamoto, A. Sato, and S. Itakura, 'Eye tracking in an everyday environment reveals the interpersonal distance that affords infant-parent gaze communication', *Sci. Reports*, vol. 9, no. 1, p. 10352, Jul. 2019, doi: 10.1038/s41598-019-46650-6.

[7] H. Heidari and V. Nabaei, *Magnetic Sensors for Biomedical Applications*. John Wiley & Sons, 2019.

[8] A. de Marcellis *et al.*, 'Giant Magnetoresistance (GMR) sensors for 0.35µm CMOS technology sub-mA current sensing', in *2014 IEEE SENSORS*, Nov. 2014, pp. 444–447, doi: 10.1109/ICSENS.2014.6985030.

[9] H. X. Wei, Q. H. Qin, M. Ma, R. Sharif, and X. F. Han, '80% tunneling magnetoresistance at room temperature for thin Al–O barrier magnetic tunnel junction with CoFeB as free and reference layers', *Journal of Applied Physics*, vol. 101, no. 9, p. 09B501, Apr. 2007, doi: 10.1063/1.2696590.

[10] S. Zuo *et al.*, 'Ultrasensitive Magnetoelectric Sensing System for pico-Tesla MagnetoMyoGraphy', *IEEE Transactions on Biomedical Circuits and Systems*, pp. 1–1, 2020, doi: 10.1109/TBCAS.2020.2998290.

[11] S. Zuo, H. Heidari, D. Farina, and K. Nazarpour, 'Miniaturized Magnetic Sensors for Implantable Magnetomyography', *Advanced Materials Technologies*, vol. 5, no. 6, p. 2000185, 2020, doi: 10.1002/admt.202000185.

[12] E. Paz, R. Ferreira, and P. P. Freitas, 'Linearization of Magnetic Sensors With a Weakly Pinned Free-Layer MTJ Stack Using a Three-Step Annealing Process', *IEEE Transactions on Magnetics*, vol. 52, no. 7, pp. 1–4, Jul. 2016, doi: 10.1109/TMAG.2016.2525772.

[13] E. Paz, S. Serrano-Guisan, R. Ferreira, and P. P. Freitas, 'Room temperature direct detection of low frequency magnetic fields in the 100 pT/Hz0.5 range using large arrays of magnetic tunnel junctions', *Journal of Applied Physics*, vol. 115, no. 17, p. 17E501, Jan. 2014, doi: 10.1063/1.4859036.

[14] P. Graybill and M. Kiani, 'Eyelid Drive System: An Assistive Technology Employing Inductive Sensing of Eyelid Movement', *IEEE Trans. Biomed. Circuits Syst.*, pp. 1–1, 2018, doi: 10.1109/TBCAS.2018.2882510.

[15] R. Paprocki and A. Lenskiy, 'What Does Eye-Blink Rate Variability Dynamics Tell Us About Cognitive Performance?', *Front. Hum. Neurosci.*, vol. 11, 2017, doi: 10.3389/fnhum.2017.00620.

[16] M. J. Cartwright, U. R. Kurumety, C. C. Nelson, B. R. Frueh, and D. C. Musch, 'Measurements of upper eyelid and eyebrow dimensions in healthy white individuals', *Am. J. Ophthalmol.*, vol. 117, no. 2, pp. 231–234, Feb. 1994, doi: 10.1016/s0002-9394(14)73081-8.

[17] M. Yuan *et al.*, 'Electronic Contact Lens: A Platform for Wireless Health Monitoring Applications', *Advanced Intelligent Systems*, vol. 2, no. 4, p. 1900190, 2020, doi: 10.1002/aisy.201900190.

[18] J. Keyes, M. Junkin, P. K. Wong, and J. P. Vande Geest, 'Computational simulation of a magnetic microactuator for tissue engineering applications', *Biomed Microdevices*, vol. 11, no. 6, pp. 1259–1267, Dec. 2009, doi: 10.1007/s10544-009-9345-1.

[19] 'International Commission on Non-Ionizing Radiation Protection: guidelines for exposure to static magnetic field', 2009. .

[20] W. Jung, *Op Amp Applications Handbook*. Newnes, 2005.

[21] S.-U. Yoon, A. Markham, N. Trigoni, T. E. Abrudan, O. Kypris, and C. Wietfeld, 'Chapter 7 - Advances and Challenges in Underground Sensing', in *Underground Sensing*, S. Pamukcu and L. Cheng, Eds. Academic Press, 2018, pp. 357–415.